

Supplementary Information

Läubli *et al*, Engagement of Myelomonocytic Siglecs by Tumor-associated Ligands
Modulates the Innate Immune Response to Cancer

Supplementary Methods

Murine tumor models. MCA was dissolved in corn oil and injected into the flank of SigE^{-/-} or wildtype control mice. Tumor appearance was monitored over time. MC38GFP and LLC cells were lifted with EDTA before injection into lateral tail veins of mice for analysis of lung nodule formation and interaction with myelomonocytic cells by fluorescence microscopy. For analysis of subcutaneous tumor growth, murine colon carcinoma cell line MC38, murine lung carcinoma cell line LLC and murine melanoma cell line B16F1 were injected into flank of mice. Depletion of neutrophils was achieved by intraperitoneal injection of 500 µL anti-Ly6G antibody (1A8, BioXCell, or isotype control IgG 2A3). Monocytes and macrophages were depleted by intravenous injection of 100 µL of clodronate containing liposomes (Encapsula NanoSciences).

Lectin staining of human cancer samples. Chimeric proteins of the first two domains of human Siglec-9 and the human Fc and an intervening Flag tag were produced by expression in 293A cells and purification with protein A beads. Frozen and formalin fixed tissue sections from different carcinomas were incubated with the chimeric Siglec-9-Fcs and biotinylated anti-Flag-tag antibodies were used to detect bound Siglec-9-Fcs.

Flow cytometry. For staining of Siglec ligands, Siglec-Fc chimeras were used. The K131QSiglec-9-Fc mutant was generated by Quick Change (Agilent). We used 2 mM IO₄⁻ in PBS on formalin fixed cells for mild oxidation of the C8 and C9 side chains of sialic acids. Sialidase from *Arthrobacter ureafaciens* (AUS) was used to remove sialic acid on cell surfaces in other experiments. Subcutaneous tumors were minced with

razor blades and treated for 30 minutes with collagenase/dispase (Roche). Anti-CD45, anti-CD11b, anti-Ly6G, anti-B220, anti-CD3, anti-NK1.1 (all from BD Biosciences) anti-F4/80, anti-CD206 (from Biolegend) were used to analyze tumor infiltrating leukocytes. For analysis of Siglec-E expression, polyclonal anti-Siglec-E was used (R&D Systems). Anti-human Siglec-9 antibodies were used to stain for Siglec-9 expression (R&D Systems, Clone #191240). Samples were analyzed with a FACS Calibur. Subcutaneous MCA tumors were also minced and treated with collagenase/dispase before putting the cells into culture for one passage and subsequently analyze Siglec-E-Fc binding by flow cytometry.

Analysis of Siglec-9 clustering on neutrophils. Freshly isolated neutrophils were co-cultured for 60 minutes on CFSE labeled LS180 or A549 adherent tumor cells. Non-adherent neutrophils were washed away and slides fixed with 3% neutral buffered formalin for 10 minutes at room temperature. Siglec-9 was stained with a polyclonal antibody (R&D Systems).

Immunostaining of mouse tissue. Sections from lung and subcutaneous tumors were obtained from in O.C.T. frozen tissue. Antibodies against murine Ly6G, CD3, CD11, CD31 (all from BD Biosciences), NK46p, Siglec-E (R&D Systems) and F4/80 (Serotec) were used for subsequent immunostaining.

Analysis of myelomonocytic cells in vitro. Human neutrophils were prepared by separation from PBMC via Ficoll gradient and subsequent dextran sedimentation. Murine neutrophils were isolated from bone marrow via Percoll density gradient. For analysis of extracellular ROS production we used the OxyBurst assay (Invitrogen). Tumor cell apoptosis was assayed after labeling tumor cells with carboxyfluorescein succinimidyl ester (CFSE, Biolegend) and intracellular staining of cleaved caspase 3 (Cell Signaling) by flow cytometry. Siglec-9 function was analyzed with a function blocking antibody (R&D Systems, clone 191240) and a non-function blocking antibody (BD Biosciences, clone E10-286). For analysis of tumor cell killing, MC38GFP cells or CFSE pre-labeled LS180 were seeded on a 96well plate overnight

and neutrophils were added at effector to target ratios at approximately 20:1 or 40:1 and fluorescent cells were quantified at different time points.

SHP recruitment assay to Siglec-9. Freshly isolated human neutrophils were co-cultured for 30 minutes on LS180 or A549 tumor cells or on empty culture dishes. Non-adherent neutrophils were washed away and cells were lysed directly on culture dishes in buffer containing 1% Nonidet-P40 and 1:50 protease inhibitor cocktail (Calbiochem), PhosStop (Roche) and micrococcal nuclease. Siglec-9 was bound to biotinylated anti-Siglec-9 IgG (R&D Systems, polyclonal, BAF1139) overnight at 4 degrees. Streptavidin-sepharose beads (GE Healthcare) were used to bind biotinylated anti-Siglec-9. Immunoprecipitates were loaded on a 10% polyacrylamide gel and blotted on a PVDF membrane. SHP-1 was detected with polyclonal anti-rabbit antibody (Santa Cruz).

Sialoglycan microarrays. Glycan microarrays were fabricated by using epoxide-derivatized slides. Binding studies of Siglec-9-Fc, R120K-Siglec-9-Fc and K131Q-Siglec-9-Fc chimeras were performed. Printed glycan microarray slides were blocked by ethanolamine, washed and dried, and then fitted in a multi-well microarray hybridization cassette (ArrayIt) to divide into subarrays. The subarrays were blocked with Ovalbumin (1% w/v) in PBS (pH 7.4) for 1 hour at RT, with gentle shaking. Subsequently, the blocking solution was removed and diluted Siglecs samples were added to each subarray. After incubating the Siglecs for 2 hours at RT with gentling shaking, the slides were extensively washed to remove non-specifically bound proteins. Fluorescently labeled antibody (Cy3-labeled goat anti-human IgG, Jackson ImmunoResearch Laboratories) was applied and incubated for 1h. Following final washes and drying, the developed sialoglycan microarray slides were subjected to scanning by using a Genepix 4000B microarray scanner (Molecular Devices Corp., Union City, CA) right away. Data analysis was done by using the Genepix Pro 7.0 analysis software (Molecular Devices Corp., Union City, CA). All Siglec chimeras, the Siglec-9-Fc, R120K-Siglec-9-Fc and K131Q-Siglec-9-Fc, were analyzed at different concentrations on the array.

Analysis of the Sialic Acid Binding Properties of Siglec-9 variants. 96-well plates (Costar) were coated overnight at 4 °C with 200 ng/well Protein A (Pierce) in 50 mM carbonate/bicarbonate buffer pH 9.5 and then blocked with 200 ml blocking buffer (20 mM HEPES pH 7.5, 1% bovine serum albumin, 125 mM NaCl, 1 mM CaCl₂, 1 mM MgCl₂) for 1 hour at room temperature. 500 ng/well of Siglec-9 Fc variants in blocking buffer were incubated for 2 hours at room temperature. Wells were washed three times with washing buffer (20 mM HEPES pH 7.5, 125 mM NaCl, 1 mM CaCl₂, 1 mM MgCl₂). Biotin-conjugated polyacrylamide substituted with Neu5Ac α 2–6Gal β 1–4Glc or Neu5Ac α 2–3Gal β 1–4GlcNAc (Glycotech) were added at various concentrations in blocking buffer for 2 hours, followed by washing and incubation with HRP-conjugated streptavidin (R&D Systems) for 1 hour. TMB (R&D Systems) was used as a substrate. Reactions were stopped with addition of H₂SO₄ and plates were read at 405 nm with a SpectraMax reader (Molecular Devices).

Isolation of bone marrow derived macrophages and peritoneal resident macrophages. For isolation of bone marrow derived macrophages, femurs and tibiae of wildtype and Siglec-E deficient mice were flushed with DMEM without serum. After enrichment of macrophages by adherence to plastic, macrophages were differentiated by culturing in L929 conditioned medium. Peritoneal macrophages were obtained by repeated flushing of the peritoneum of wildtype and Siglec-E deficient mice with icecold PBS. Peritoneal macrophages were treated by 10 ng/mL IL4, 100 ng/mL LPS or co-cultured with MC38-GFP tumor cells for 2 days and polarization analyzed by staining with anti-CD206 (Biolegend) or anti-CCR2 (BD Biosciences) antibodies. Siglec-E expression on macrophages were determined by a polyclonal anti-Siglec-E antibody (R&D Systems).

Polarization of human monocyte-derived macrophages. Human macrophages were obtained by adherence of PBMC to a cell culture dish for 3 hours in RPMI-1640 without serum and differentiated over 7 days in RPMI-1640 containing 10% FCS, penicillin/streptomycin and 100 ng/mL M-CSF. Control polarization to M2 was

performed by adding 20 ng/mL of IL4 to fresh RPMI-1640, 10% FCS medium for 48 hours. LS180 was added at 5×10^5 per mL for direct co-culture and blocking or non-blocking anti-Siglec-9 at 25 μ g/mL. Polarization was measured by percent of CD206 of CD14 positive cells in co-culture by flow cytometry. CD33 related Siglec expression on monocyte-derived macrophages was determined by staining with anti-Siglec-3, -7 -9 (R&D Systems) and anti-Siglec-5 (Biolegend) antibodies on CD14 positive cells.

Statistical analysis. For analysis of statistical significance between two groups a two-tailed Student's *t* test was used. For the testing significance between more than two conditions, a one-way ANOVA with multiple comparisons was used, while for growth curves and analyses over time were tested with a two-way ANOVA analysis. Descriptive patient data was analyzed by two-tailed *t* or chi-square tests. Data points were usually presented as mean \pm SEM, unless otherwise stated in the figure legends. Logistic regression for estimating non-small cell lung cancer risk in total sample and emphysema risk among NSCLC cases was used. The genotype effects were estimated assuming an additive genetic model (0, 1 or 2 copies of minor allele). Cox proportional hazards models were used for estimating mortality risk among non-small cell lung cancer cases. The genotype effects were estimated as one or two copies of minor allele versus zero copies of minor allele. A P value <0.05 was considered as significant.

Supplementary Figures and Tables

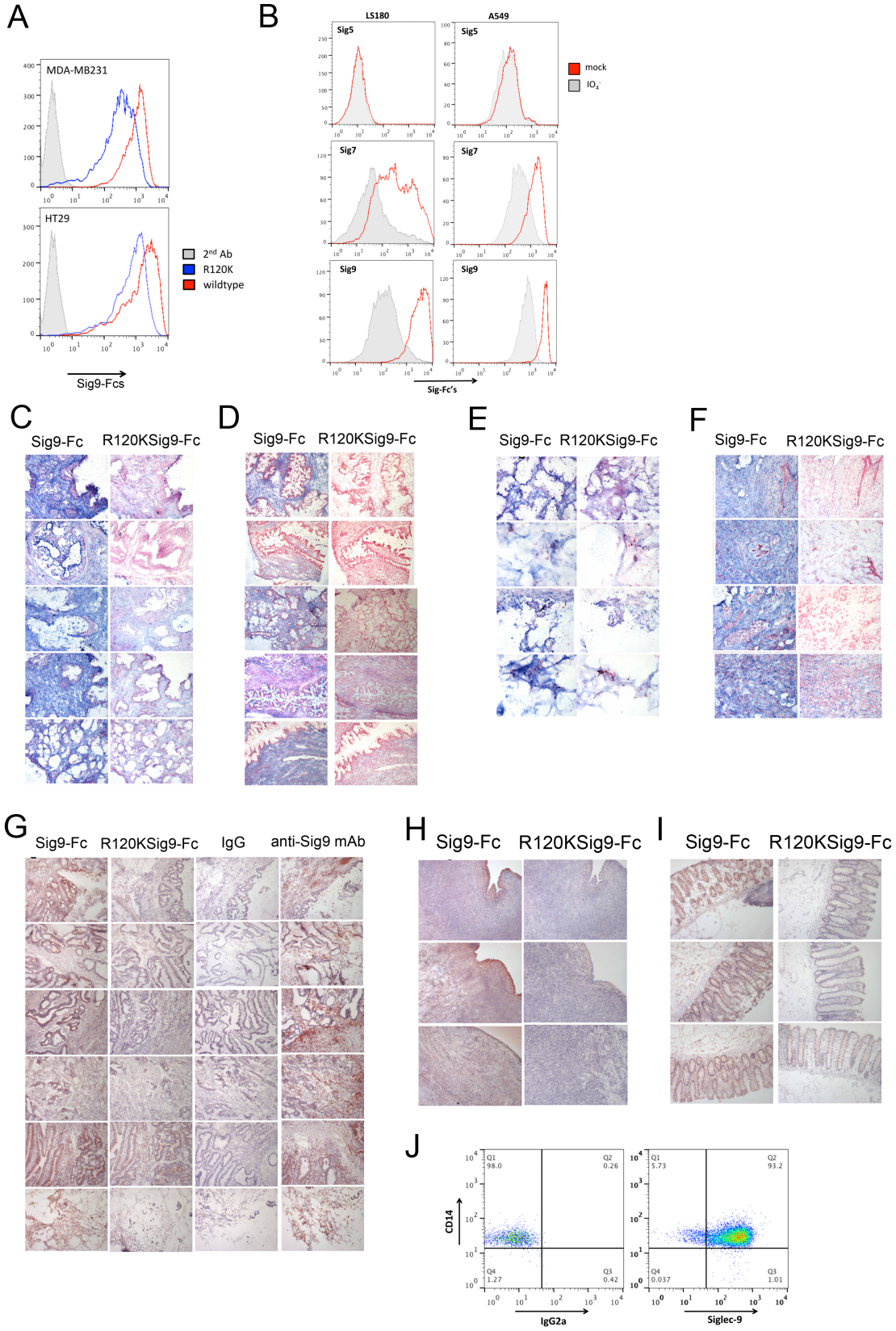


Figure S1 (A) Tumor cells were labeled with either the Siglec-9-Fc or the R120K-Siglec-9-Fc chimera and analyzed by flow cytometry. (B) LS180 and A549 cells were stained with Siglec-Fc chimeras of Siglec-5, -7 and -9. (C), ovarian (D), non-small cell lung (E), breast (F) and colorectal (G) cancer samples were stained for Siglec-9 ligands with Siglec-9-Fc and R120K-Siglec-9-Fc chimeras and also in E with anti-Siglec-9 antibody. Healthy ovary (H) or colon tissue (I) stained with Siglec-9-Fc or R120K-Siglec-9-Fc chimera. Magnification 200x for all histology images. (J) Analysis of Siglec-9 expression on tumor infiltrating myeloid cells in a sample of human colorectal cancer by flow cytometry. Gated on CD11b, all the CD14 positive cells are also Siglec-9 positive (IgG2A, isotype control, left panel).

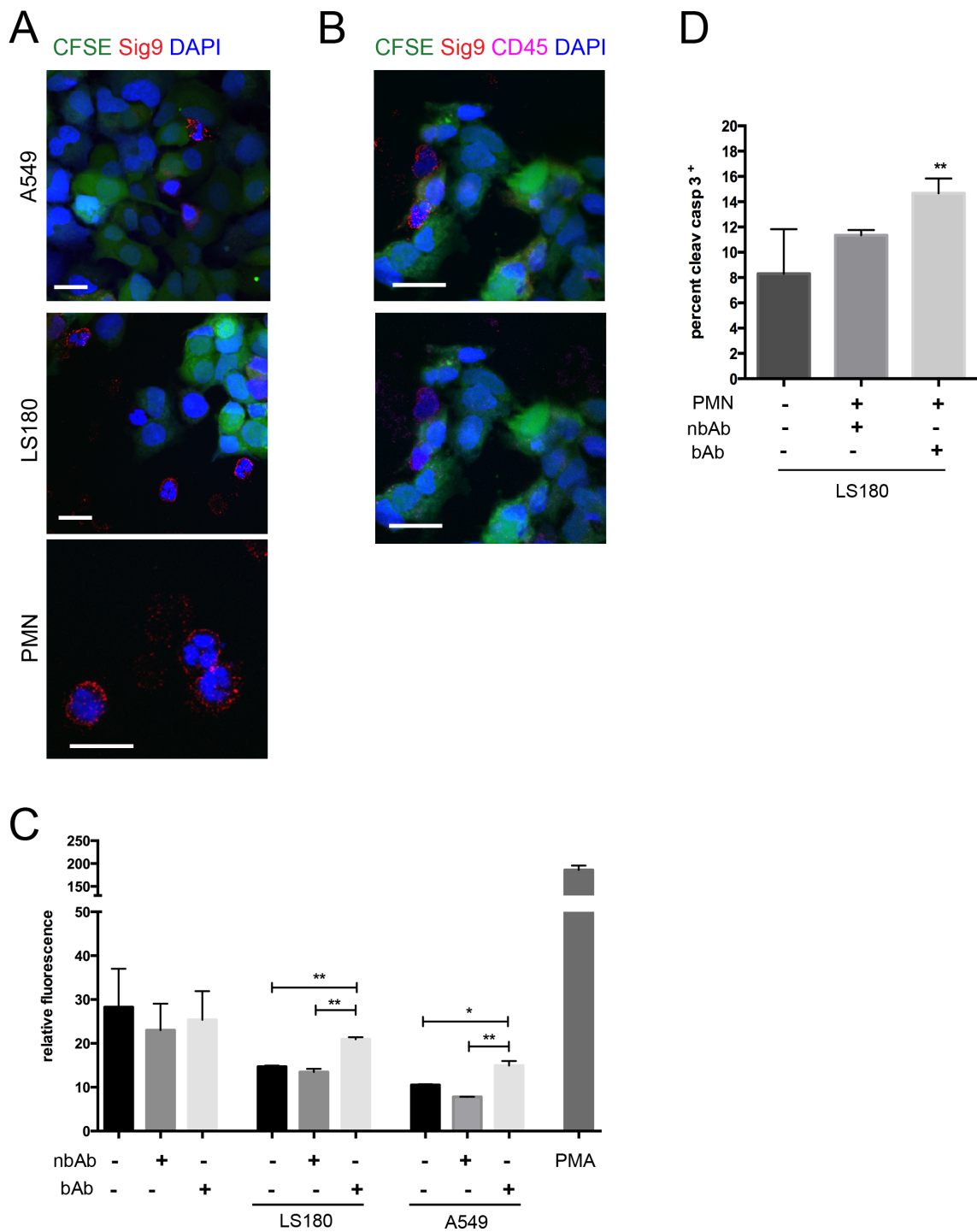


Figure S2 (A) Co-incubation of A549 or LS180 cells (CFSE stained, green) for 60 minutes with freshly isolated human neutrophils and stained for Siglec-9 (red) DNA with DAPI (blue). **(B)** Co-incubation of LS180 cells (CFSE stained, green) for 60 minutes with human neutrophils stained for Siglec-9 (red, upper panel) and CD45

(magenta, lower panel). Nuclei stained with DAPI (blue). Scale bar, 20 μm . **(C)** ROS release by human neutrophils incubated with LS180 or A549 tumor cells. ROS levels were analyzed by increase of fluorescence using Oxyburst assay, (N=3), in presence or absence of non-blocking anti-Siglec-9 antibody (nbAb, E10-286) or blocking anti-Siglec-9 antibody (bAb, 191240) both used at 25 $\mu\text{g}/\text{mL}$. Phorbol myristate acetate (PMA, 1 $\mu\text{g}/\text{mL}$) was used to activate neutrophils. **(D)** Determination of cleaved caspase 3 positive LS180 cells 6 hours after incubation with 40:1 neutrophils (effector:target) by flow cytometry. Tumor cells were stained with CFSE prior to the assay (N=3-4). * $P < 0.05$, ** $P < 0.01$.

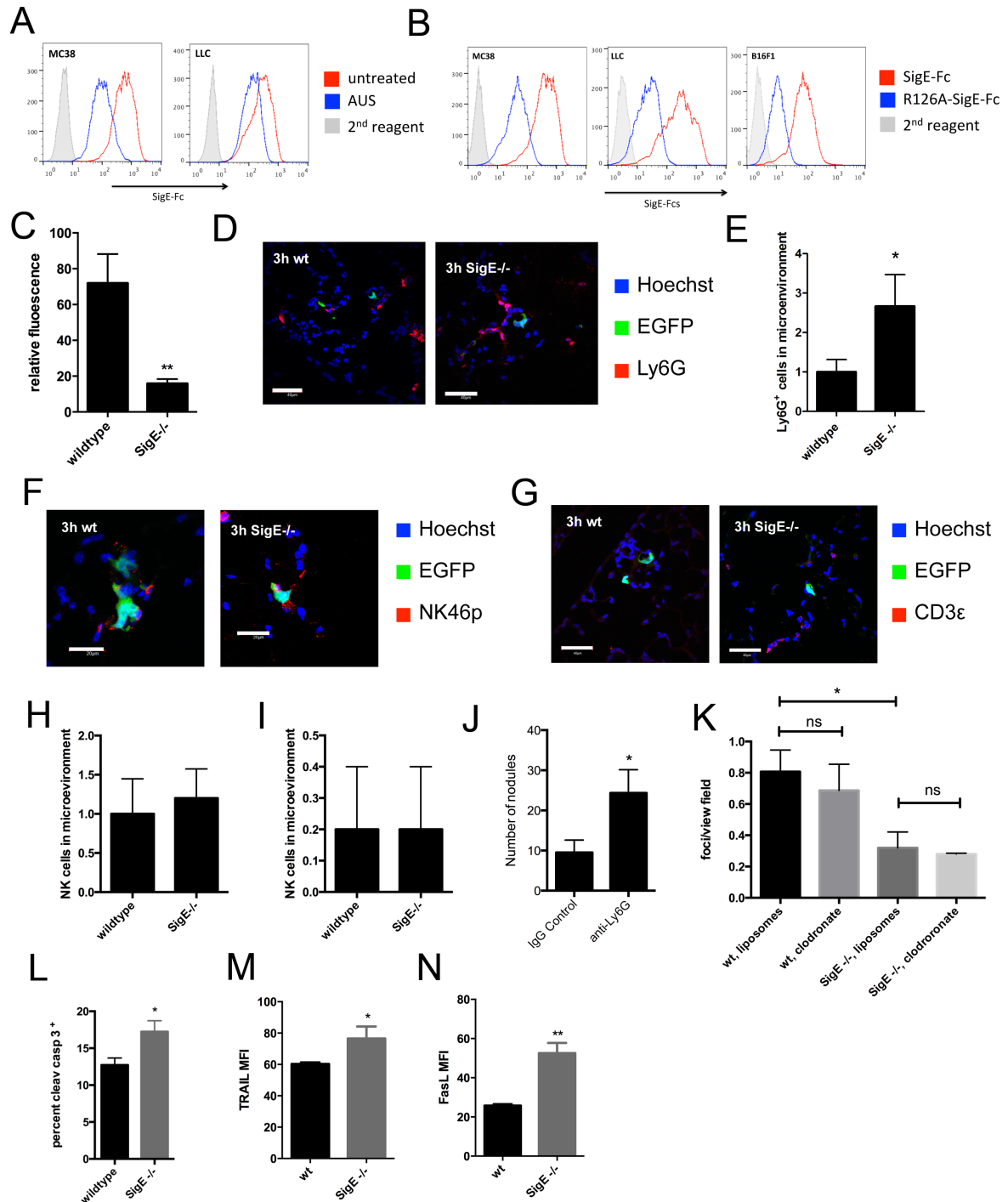


Figure S3 (A) MC38 and LLC tumor cells labeled for Siglec-E ligands by Siglec-E-Fc chimera treated or untreated with sialidase (AUS, *A. ureafaciens* sialidase). **(B)** MC38, LLC and B16F1 studied for expression of Siglec-E ligands with SigE-Fc or Arg-mutant R126ASigE-Fc chimera (produced by site directed mutagenesis). **(C)**

GFP measurement in homogenized lungs from SigE^{-/-} and wildtype mice 21 days after i.v. injection of MC38-GFP cells. (N=9-10). **(D)** Representative images of Ly6G neutrophils in close contact to MC38-GFP cells in lungs of SigE^{-/-} and wildtype control mice 3 hours after intravenous injection. Scale bar, 40 μ m. **(E)** Quantification of Ly6G⁺ neutrophils from D (N=5). Representative images of NK46p⁺ NK cells **(F)** or CD3⁺ T cells **(G)** in lungs of SigE^{-/-} or wildtype mice 3 hours after intravenous injection of MC38-GFP cells. Scale bar F, 20 μ m, G, 40 μ m. **(H)** and **(I)** Quantification of NK cells and CD3 positive cells in close proximity of GFP positive MC38 foci (N=5). **(J)** Depletion of neutrophils by single i.p. injection of anti-Ly6G 48h before intravenous injection of syngeneic MC38 tumor cells in SigE^{-/-} mice. Analysis of nodules after 21d in lungs. **(K)** SigE^{-/-} or wildtype mice depleted of macrophages with clodronate liposomes 2 days before intravenous injection of MC38-GFP cells. Metastatic foci were counted by microscopic analysis of GFP cells 6 hours after intravenous injection. (N=4). **(L)** Measurement of cleaved caspase 3 (by flow cytometry, percentage positive) in LLC tumor cells after 6 hours co-incubation with BM derived neutrophils from wildtype and SigE^{-/-} mice. **(M)** BM derived neutrophils from wildtype and SigE^{-/-} mice after co-culture with MC38-GFP were studied for TRAIL and FasL **(N)** expression (MFI, mean fluorescence intensity, N=3). * P<0.05, ** P<0.01.

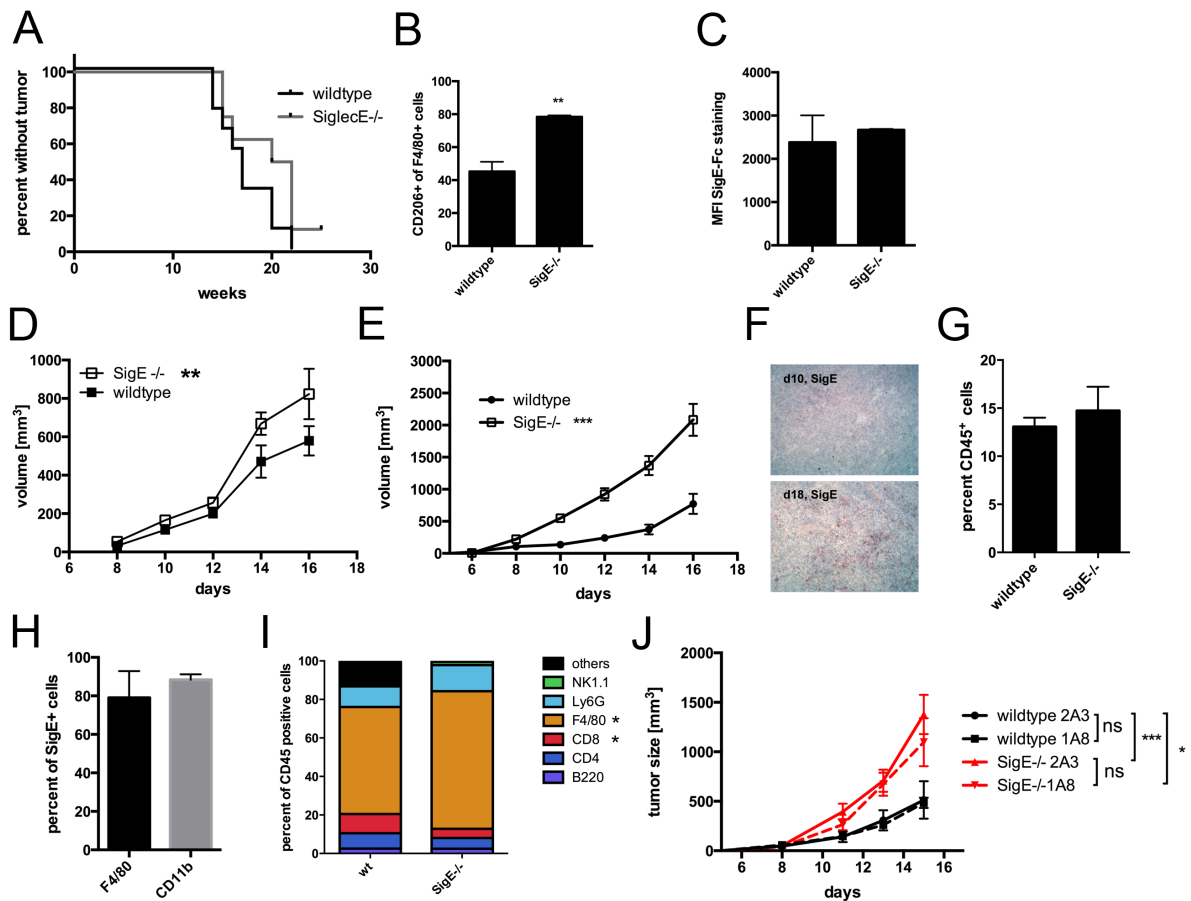


Figure S4 (A) Percent of SigE^{-/-} or wildtype mice without subcutaneous tumors after injection of 30 μ g of MCA. **(B)** Analysis of macrophage polarization in subcutaneous MCA tumors 18 weeks after injection of the carcinogen in wildtype or SigE^{-/-} mice. Tumors were minced and collagenase/dispase treated and then stained for F4/80 and CD206 before analyzed by flow cytometry (N=3-4). **(C)** Siglec-E-Fc staining of tumor cell lines obtained from MCA tumor of SigE^{-/-} and wildtype control mice (N=3). **(D)** Growth curve of LLC tumors after subcutaneous injection in SigE^{-/-} and wildtype littermate control mice (N=8). **(E)** Growth curve of subcutaneous B16F1 tumors in SigE^{-/-} and wildtype mice (N=6-8). **(F)** Siglec-E staining in subcutaneous MC38 tumors 10 and 18 days after subcutaneous injection of tumor cells in wildtype mice. Magnification 200x. **(G)** Analysis of leukocyte infiltrates in subcutaneous MC38 tumors of SigE^{-/-} and wildtype mice by CD45 staining and flow cytometry (N=4-5). No significant difference was found by Student's *t* test. **(H)** Flow cytometric analysis of Siglec-E positive cells at day 18 in subcutaneous MC38 tumors with co-staining with

macrophage F4/80 marker and CD11b myelomonocytic marker (N=4-5). No significant difference was found by Student's *t* test. (I) Characterization of tumor infiltrating CD45 positive leukocytes in subcutaneous MC38 tumors by flow cytometry. (J) Growth of subcutaneous MC38 tumors in SigE^{-/-} and wildtype mice neutrophil depleted at day 8 with 500 µg anti-Ly6G (1A8) i.p. or treated with isotype control IgG (2A3). * P<0.05, ** P<0.01, *** P<0.001.

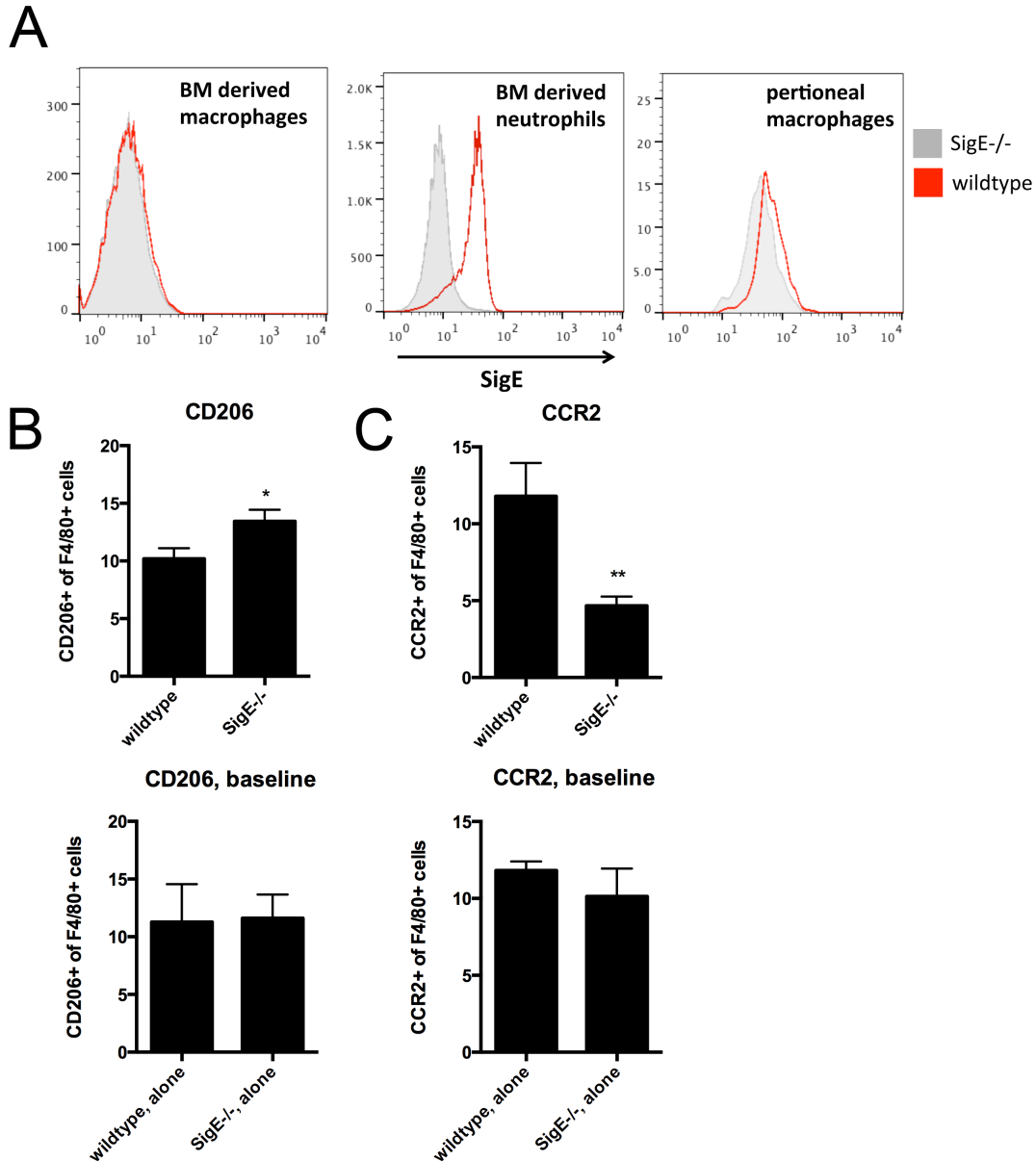


Figure 5 (A) Analysis of Siglec-E expression on different isolated myelomonocytic cell populations including bone marrow (BM) derived macrophages, BM derived neutrophils or peritoneal macrophages by flow cytometry and after staining with a polyclonal Siglec-E antibody. As negative control, cells from SigE^{-/-} mice were used. (B) and (C) Polarization analysis of peritoneal macrophages from wildtype or SigE^{-/-} after co-culture with MC38 tumor cells for 2 days. CD206 (M2, B) and CCR2 (M1, C) were used as polarization markers. Lower panels show baseline expression of M1 and M2 markers on isolated peritoneal macrophages (N=3). * P<0.05, ** P<0.01.

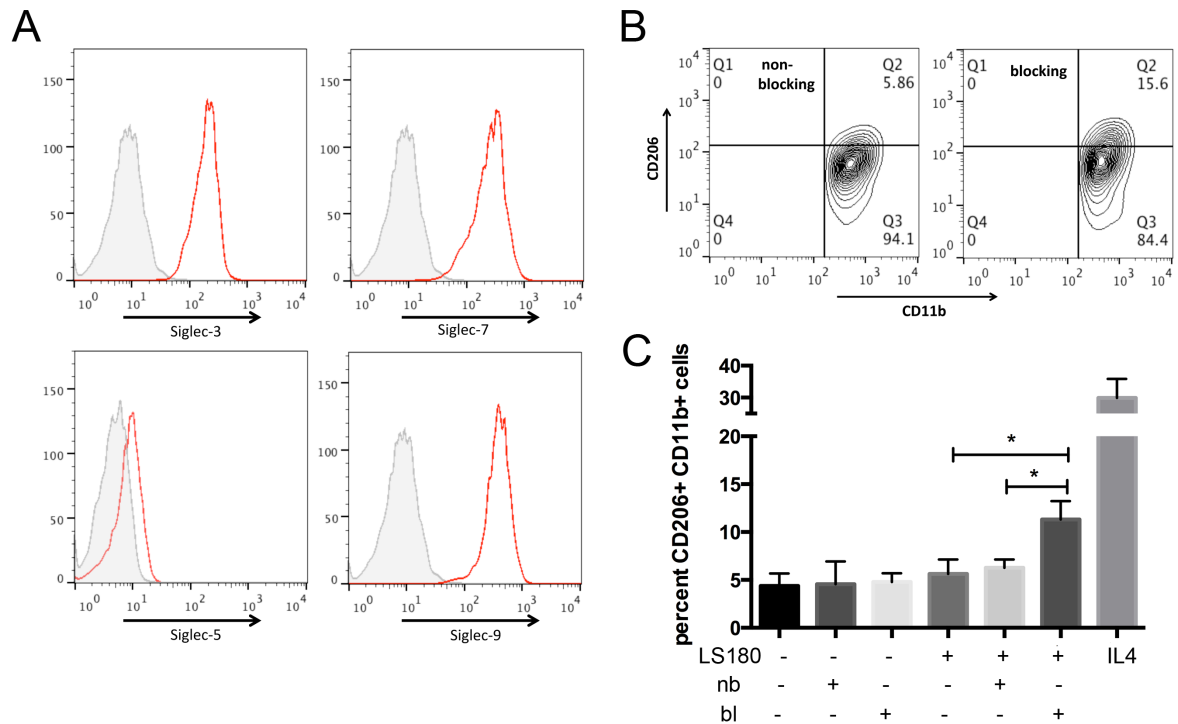


Figure S6 (A) Analysis of Siglec-3, -5, -7 and 9 expression (red) on human monocyte derived macrophages by flow cytometry after 7 days of differentiation. Representative histograms of 3 independent analysis from 3 different donors (grey, isotype control). **(B)** Co-culture of LS180 tumor cells with human monocyte-derived macrophages in the presence of a non-blocking or blocking anti-Siglec-9 antibody for 48 hours and analysis of CD206+ CD11b+ cells. **(C)** Statistical analysis of flow cytometric data of co-culture of human monocyte-derived macrophages with LS180 tumor cells (nb, non-blocking; bl, blocking anti-Siglec-9 antibody, N=3-4). * P<0.05 by Student's *t* test.

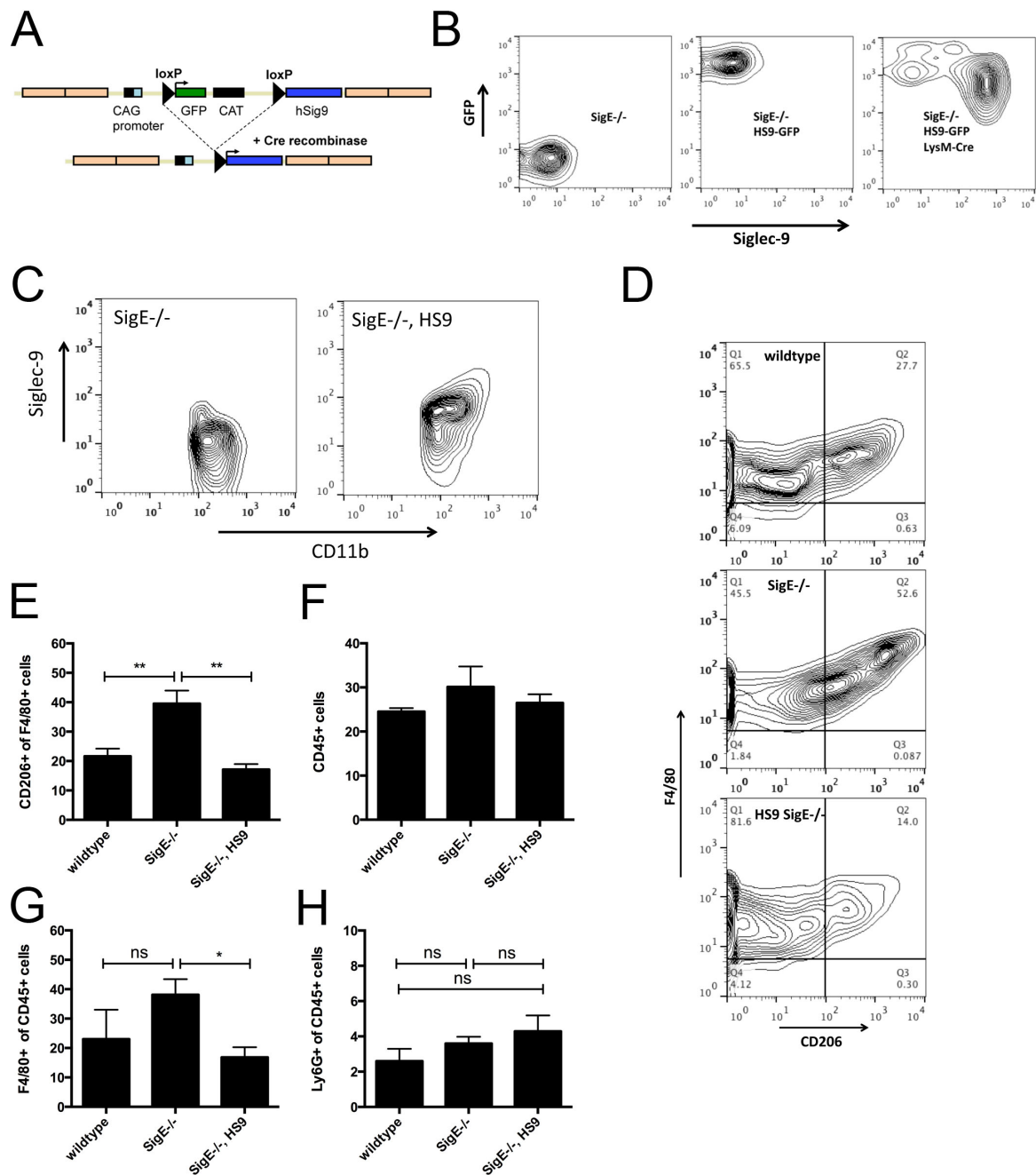


Figure S7 (A) Schematic representation of transgenic expression of human Siglec-9. **(B)** Analysis of human Siglec-9 expression in peripheral blood neutrophils of SigE^{-/-} mice, SigE^{-/-} HS9-GFP transgenic mice and mice that had the stop codon upstream of human Siglec-9 removed by expression of Cre recombinase under the LysM promoter. **(C)** Analysis of Siglec-9 expression on CD11b positive cells in subcutaneous MC38 tumors 18 days after injection in SigE^{-/-} and SigE^{-/-}, Siglec-9

transgenic mice. **(D)** Flow cytometric analysis of tumor infiltrating CD11b⁺ F4/80⁺ C206⁺ cells in subcutaneous MC38 tumors grown in wildtype, SigE^{-/-} and human Siglec-9 transgenic mice in SigE^{-/-} background. Statistical analysis of tumor infiltrating CD11b⁺ F4/80⁺ CD206⁺ **(E)**, CD45⁺ **(F)**, CD45⁺ F4/80⁺ **(G)** and CD45⁺ Ly6G⁺ **(H)** cells in subcutaneous tumors 18 days after MC38 tumor cell injection (N=3-4). * P<0.05, ** P<0.01.

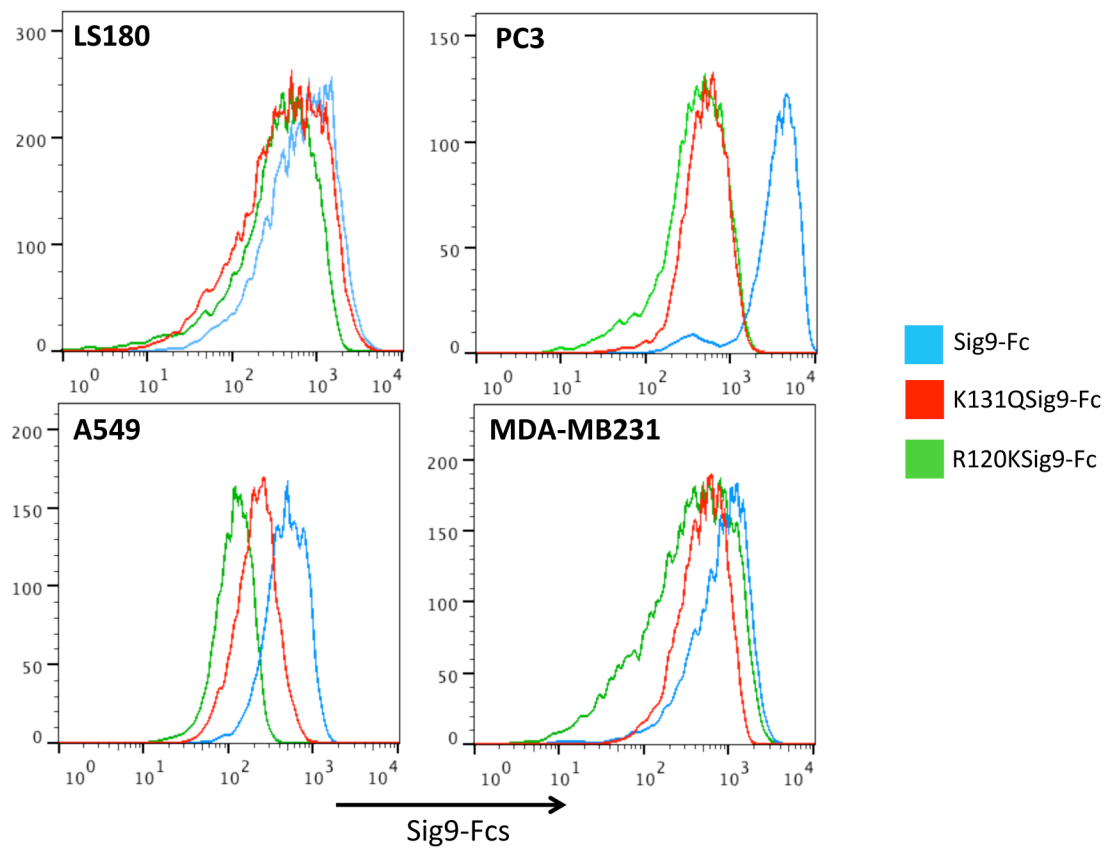


Figure S8 LS180 colorectal cancer, PC3 prostate cancer, A549 NSCLC and MDA-MB231 breast cancer cell lines stained with Siglec-9-Fc, K131Q-Siglec-9-Fc and R120K-Siglec-9-Fc chimeras.

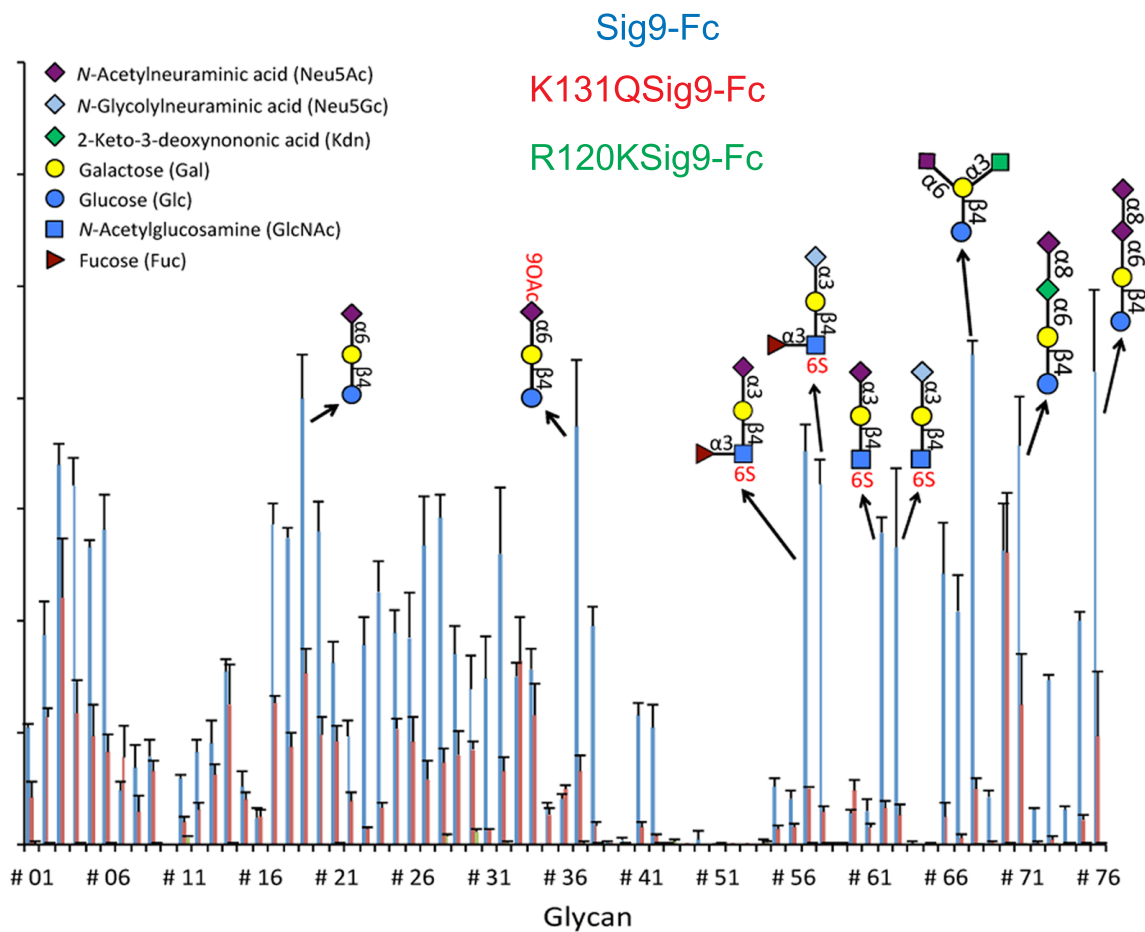


Figure S9 Binding of Siglec-9-Fc chimeras to sialoglycan array.

Glycan structure	ID	Siglecs binding			Rank
		Siglec 9	Sig9-K131Q	Sig9-R120K	
Neu5,9Ac ₂ α3Galβ4GlcNAcβO(CH ₂) ₃ NH ₂	# 01				
Neu5Gc9Aca3Galβ4GlcNAcβO(CH ₂) ₃ NH ₂	# 02				100
Neu5,9Ac ₂ α6Galβ4GlcNAcβO(CH ₂) ₃ NH ₂	# 03				
Neu5Gc9Aca6Galβ4GlcNAcβO(CH ₂) ₃ NH ₂	# 04				50
Neu5Aca6GalNAcaO(CH ₂) ₃ NH ₂	# 05				
Neu5Gca6GalNAcaO(CH ₂) ₃ NH ₂	# 06				0
Neu5,9Ac ₂ α3Galβ3GlcNAcβO(CH ₂) ₃ NH ₂	# 07				
Neu5Gc9Aca3Galβ3GlcNAcβO(CH ₂) ₃ NH ₂	# 08				
Neu5,9Ac ₂ α3Galβ3GalNAcaO(CH ₂) ₃ NH ₂	# 09				
Neu5Gc9Aca3Galβ3GalNAcaO(CH ₂) ₃ NH ₂	# 10				
Neu5Aca3Galβ4GlcNAcβO(CH ₂) ₃ NH ₂	# 11				
Neu5Gca3Galβ4GlcNAcβO(CH ₂) ₃ NH ₂	# 12				
Neu5Aca3Galβ3GlcNAcβO(CH ₂) ₃ NH ₂	# 13				
Neu5Gca3Galβ3GlcNAcβO(CH ₂) ₃ NH ₂	# 14				
Neu5Aca3Galβ3GalNAcaO(CH ₂) ₃ NH ₂	# 15				
Neu5Gca3Galβ3GalNAcaO(CH ₂) ₃ NH ₂	# 16				
Neu5Aca6Galβ4GlcNAcβO(CH ₂) ₃ NH ₂	# 17				
Neu5Gca6Galβ4GlcNAcβO(CH ₂) ₃ NH ₂	# 18				
Neu5Aca6Galβ4GlcβO(CH ₂) ₃ NH ₂	# 19				
Neu5Gca6Galβ4GlcβO(CH ₂) ₃ NH ₂	# 20				
Neu5Aca3Galβ4GlcβO(CH ₂) ₃ NH ₂	# 21				
Neu5Gca3Galβ4GlcβO(CH ₂) ₃ NH ₂	# 22				
Neu5,9Ac ₂ α6GalNAcaO(CH ₂) ₃ NH ₂	# 23				
Neu5Gc9Aca6GalNAcaO(CH ₂) ₃ NH ₂	# 24				
Neu5Aca3GalβO(CH ₂) ₃ NH ₂	# 25				
Neu5Gca3GalβO(CH ₂) ₃ NH ₂	# 26				
Neu5Aca6GalβO(CH ₂) ₃ NH ₂	# 27				
Neu5Gca6GalβO(CH ₂) ₃ NH ₂	# 28				
Neu5,9Ac ₂ α3GalβO(CH ₂) ₃ NH ₂	# 29				
Neu5Gc9Aca3GalβO(CH ₂) ₃ NH ₂	# 30				
Neu5,9Ac ₂ α6GalβO(CH ₂) ₃ NH ₂	# 31				
Neu5Gc9Aca6GalβO(CH ₂) ₃ NH ₂	# 32				
Neu5Aca3Galβ3GalNAcβO(CH ₂) ₃ NH ₂	# 33				
Neu5Gca3Galβ3GalNAcβO(CH ₂) ₃ NH ₂	# 34				
Neu5,9Ac ₂ α3Galβ3GalNAcβO(CH ₂) ₃ NH ₂	# 35				
Neu5Gc9Aca3Galβ3GalNAcβO(CH ₂) ₃ NH ₂	# 36				
Neu5,9Ac ₂ α6Galβ4GlcβO(CH ₂) ₃ NH ₂	# 37				
Neu5Gc9Aca6Galβ4GlcβO(CH ₂) ₃ NH ₂	# 38				
Neu5,9Ac ₂ α3Galβ4GlcβO(CH ₂) ₃ NH ₂	# 39				
Neu5Gc9Aca3Galβ4GlcβO(CH ₂) ₃ NH ₂	# 40				
Neu5Aca8Neu5Aca3Galβ4GlcβO(CH ₂) ₃ NH ₂	# 41				
Neu5Aca8Neu5Aca8Neu5Aca3Galβ4GlcβO(CH ₂) ₃ NH ₂	# 42				
Galβ4GlcβO(CH ₂) ₃ NH ₂	# 43				
Galβ4GlcNAcβO(CH ₂) ₃ NH ₂	# 45				
GalNAcaO(CH ₂) ₃ NH ₂	# 47				
Galβ3GalNAcβO(CH ₂) ₃ NH ₂	# 51				
Galβ3GalNAcaO(CH ₂) ₃ NH ₂	# 52				
Galβ3GlcNAcβO(CH ₂) ₃ NH ₂	# 53				
Galβ4GlcNAc6SβO(CH ₂) ₃ NH ₂	# 54				
Neu5Aca3Galβ4(Fuca3)GlcNAcβO(CH ₂) ₃ NH ₂	# 55				
Neu5Gca3Galβ4(Fuca3)GlcNAcβO(CH ₂) ₃ NH ₂	# 56				
Neu5Aca3Galβ4(Fuca3)GlcNAc6SβO(CH ₂) ₃ NH ₂	# 57				
Neu5Gca3Galβ4(Fuca3)GlcNAc6SβO(CH ₂) ₃ NH ₂	# 58				
Galβ3GlcNAcβ3Galβ4GlcβO(CH ₂) ₃ NH ₂	# 59				
Neu5Aca3Galβ3GlcNAcβ3Galβ4GlcβO(CH ₂) ₃ NH ₂	# 60				
Neu5Gca3Galβ3GlcNAcβ3Galβ4GlcβO(CH ₂) ₃ NH ₂	# 61				
Neu5Aca3Galβ4GlcNAc6SβO(CH ₂) ₃ NH ₂	# 62				
Neu5Gca3Galβ4GlcNAc6SβO(CH ₂) ₃ NH ₂	# 63				
Neu5Aca8Neu5Aca3Galβ4GlcβO(CH ₂) ₃ NHCOCH ₂ (OCH ₂ CH ₂) ₆ NH ₂	# 64				
Neu5Aca8Neu5Aca8Neu5Aca3Galβ4GlcβO(CH ₂) ₃ NHCOCH ₂ (OCH ₂ CH ₂) ₆ NH ₂	# 65				
Neu5Aca6(Neu5Aca3)Galβ4GlcβO(CH ₂) ₃ NH ₂	# 66				
Neu5Aca6(Neu5Gca3)Galβ4GlcβO(CH ₂) ₃ NH ₂	# 67				
Neu5Aca6(Kdna3)Galβ4GlcβO(CH ₂) ₃ NH ₂	# 68				
Neu5Gca8Neu5Aca3Galβ4GlcβO(CH ₂) ₃ NH ₂	# 69				
Kdna8Neu5Aca3Galβ4GlcβO(CH ₂) ₃ NH ₂	# 70				
Neu5Aca8Kdna6Galβ4GlcβO(CH ₂) ₃ NH ₂	# 71				
Neu5Aca8Neu5Gca3Galβ4GlcβO(CH ₂) ₃ NH ₂	# 72				
Neu5Aca8Neu5Gca6Galβ4GlcβO(CH ₂) ₃ NH ₂	# 73				
Kdna8Neu5Gca3Galβ4GlcβO(CH ₂) ₃ NH ₂	# 74				
Neu5Gca8Neu5Gca3Galβ4GlcβO(CH ₂) ₃ NH ₂	# 75				
Neu5Aca8Neu5Aca6Galβ4GlcβO(CH ₂) ₃ NH ₂	# 76				

Figure S10 Heat map of binding of different Sig9-Fc chimeras to different sialoglycans (structure on the left side) on the microarray.

Table S1

Sample description of 699 African Americans genotyped for rs16988910

Variable	Cases (n=332)	Controls (n=367)	Test of Homogeneity
Gender			
Male	146	153	0.542
Female	186	214	
Age (mean, SD)	61.6 (10.5)	60.7 (10.8)	0.287
Emphysema (unadjusted)			
No	200	367	<0.001
Yes	132	0	
Education years (mean, SD)	12.2 (2.6)	12.9 (2.3)	<0.001
Family history of lung cancer			
No	274	328	0.009
Yes	58	39	
Smoking status			
Never	14	17	0.790
Ever	318	350	
Packyears (smokers only) (mean, SD)	36.4 (26.8)	30.4 (20.8)	0.001

Table S2

Descriptive statistics for African American NSCLC cases, by rs16988910 genotype

Variable	rs16988910		Test of Homogeneity
	0 copies of minor allele (n=142)	1 or 2 copies of minor allele (n=181)	
Stage			
Local	34	53	0.426
Regional	36	52	
Distant	67	75	
Histology			
Squamous	39	43	0.647
Adenocarcinoma	77	113	
Large cell	5	5	
Other	4	3	
NSCLC (NOS)	17	17	
Surgery			
No	91	104	0.250
Yes	51	76	

Table S3

Association of non-small cell lung cancer risk and emphysema risk (among NSCLC cases) with rs16988910 genotype

Minor allele	MARF‡	Lung cancer*		Emphysema**	
		OR (95%CI)	<i>p</i> -value	OR (95%CI)	<i>p</i> -value
C	0.307	1.14 (0.90, 1.44)	0.280	1.49 (1.05, 2.11)	0.027

*Model for lung cancer risk adjusted for pack-years, education years and family history of lung cancer

**Model for emphysema risk among cases adjusted for pack-years, education years, age and gender

‡Minor allele relative frequency estimated in controls only